Test Models for Statistical Inference: Two-Dimensional Reaction Systems Displaying Limit Cycle Bifurcations and Bistability

Tomislav Plesa, Tomáš Vejchodský, Radek Erban

Abstract

Theoretical results regarding two-dimensional ordinary-differential equations (ODEs) with second-degree polynomial right-hand sides are summarized, with a focus on multistability, limit cycles and limit cycle bifurcations. The results are then used for construction of two reaction systems, which are at the deterministic level described by two-dimensional third-degree kinetic ODEs. The first system displays a homoclinic bifurcation, and a coexistence of a stable critical point and a stable limit cycle in the phase plane. The second system displays a multiple limit cycle bifurcation, and a coexistence of two stable limit cycles. The deterministic solutions (obtained by solving the kinetic ODEs) and stochastic solutions (obtained by generating noisy time-series using the Gillespie algorithm) of the constructed systems are compared, and the observed differences highlighted. The constructed systems are proposed as test problems for statistical methods, which are designed to detect and classify properties of given noisy time-series arising from biological applications.

1 Introduction

The inverse problem consisting of mapping given noisy time-series to compatible reaction networks is of importance when the possible biological mechanisms underlying the time-series are of interest [1]. Reaction networks compatible with given noisy time-series may be induced from the deterministic kinetic ordinary-differential equations (ODEs) which are compatible with the time-series [2]. However, in order to match suitable deterministic kinetic equations with given stochastic time-series, it is important to determine the type of the deterministic stable invariant sets which are 'hidden' in the time-series. This may be a challenging task, especially when cycles (oscillations) are observed in the time-series. The observed cycles can be classified as mixed (also known at the stochastic level as *noisy deterministic cycles*), which are present in both the deterministic and stochastic models, or as purely stochastic (also known as *quasi-cycles*, or noise-induced oscillations), present only in the stochastic model. Noisy deterministic cycles

may arise directly from the autonomous kinetic ODEs, or via the time-periodic terms present in the nonautonomous kinetic ODEs. Quasi-cycles may arise from the intrinsic or extrinsic noise, and have been shown to exist near deterministic stable foci, and even near deterministic stable nodes [3]. For two-species reaction systems, quasi-cycles can be further classified into those that are unconditionally noise-dependent (but dependent on the reaction rate coefficients), and those that are conditionally noise-dependent [3]. Thus, a cycle detected in a noisy time-series may at the deterministic level generally correspond to a stable limit cycle, a stable focus, or a stable node.

In order to detect and classify cycles in noisy time-series, several statistical methods have been suggested [1, 4]. For example, in [1], analysis of the covariance as a function of the time-delay, spectral analysis (the Fourier transform of the covariance function), and analysis of the shape of the stationary probability mass function, have been suggested, first two of which rely on how long the stochastic state spends near the suspected cycle, which can be a limitation if stochastic switching is present. Let us note that reaction networks of the Lotka-Volterra type are used as test models in [1], and that conditionally noise-dependent quasi-cycles, which can arise near a stable node, and which can induce oscillations in only a subset of species [3], have not been discussed. In addition to the aforementioned statistical methods developed for analysing noisy time-series, analytical methods for locally studying the underlying stochastic processes near the deterministic critical points and limit cycles, for a fixed reaction network, have also been developed [3, 5, 6, 7, 8, 9].

Statistical and analytical methods for studying cycles in stochastic reaction kinetics have been often focused on deterministically monostable systems which undergo a local bifurcation near a critical point, known as the supercritical Hopf bifurcation. We suspect this is partially due to the simplicity of the bifurcation, and partially due to the fact that it is difficult to find two-species reaction systems, which are more amenable to mathematical analysis, undergoing more complicated bifurcations and displaying bistability involving stable limit cycles. Nevertheless, more complicated bifurcations and structures in the phase space of the kinetic ODEs arising in biology can be found (see e.g. [10]), and it is, thus, of importance to test the available methods on simpler test models that display some of the complexities found in the applications.

In this paper, we construct two reaction systems that are two-dimensional (i.e. they only include two chemical species) and induce cubic kinetic equations, first of which undergoes a global bifurcation known as a convex supercritical homoclinic bifurcation, and which displays bistability involving a critical point and a limit cycle (which we call mixed bistability). The second system undergoes a local bifurcation known as a multiple limit cycle bifurcation, and displays bistability involving two limit cycles (which we call bicyclicity). Aside from finding an application as test models for statistical

inference and analysis in biology, to our knowledge, the constructed systems are also the first examples of two-dimensional reaction systems displaying the aforementioned types of bifurcations and bistabilities.

The reaction network corresponding to the first system is given by

$$\begin{aligned}
r_1 &: \quad \varnothing \xrightarrow{k_1} s_1, & r_7 &: \quad \varnothing \xrightarrow{k_7} s_2,\\
r_2 &: \quad s_1 \xrightarrow{k_2} 2s_1, & r_8 &: \quad s_2 \xrightarrow{k_8} \varnothing,\\
r_3 &: \quad 2s_1 \xrightarrow{k_3} 3s_1, & r_9 &: \quad s_1 + s_2 \xrightarrow{k_9} s_1 + 2s_2,\\
r_4 &: \quad s_1 + s_2 \xrightarrow{k_4} s_2, & r_{10} &: \quad 2s_2 \xrightarrow{k_{10}} 3s_2,\\
r_5 &: \quad 2s_1 + s_2 \xrightarrow{k_5} s_1 + s_2, & r_{11} &: \quad 3s_2 \xrightarrow{k_{11}} 2s_2,\\
r_6 &: \quad s_1 + 2s_2 \xrightarrow{k_6} 2s_1 + 2s_2, & & \qquad (1)
\end{aligned}$$

where the two species s_1 and s_2 react according to the eleven reactions $r_1, r_2, \ldots, r_{11}$ under the mass-action kinetics, with the reaction rate coefficients denoted $k_1, k_2, \ldots, k_{11}$, and with $\varnothing$ being the zero-species [2]. A particular choice of the (dimension-less) reaction rate coefficients is given by

$$\begin{aligned}
&k_1 = 0.01, \quad k_2 = 0.9, \quad k_3 = 1.55, \quad k_4 = 2.6, \quad k_5 = 1.2, \quad k_6 = 1.5,\\
&k_7 = 0.01, \quad k_8 = 3.6, \quad k_9 = 1, \quad k_{10} = 2.4, \quad k_{11} = 0.8, \qquad (2)
\end{aligned}$$

while more general conditions on these parameters are derived later as equations (10) and (11).

The reaction network corresponding to the second system includes two species s_1 and s_2 which are subject the following fourteen chemical reactions $r_1, r_2, \ldots, r_{14}$:

$$\begin{aligned}
r_1 &: \quad \varnothing \xrightarrow{k_1} s_1, & r_8 &: \quad \varnothing \xrightarrow{k_8} s_2,\\
r_2 &: \quad s_1 \xrightarrow{k_2} \varnothing, & r_9 &: \quad s_2 \xrightarrow{k_9} 2s_2,\\
r_3 &: \quad 2s_1 \xrightarrow{k_3} 3s_1, & r_{10} &: \quad s_1 + s_2 \xrightarrow{k_{10}} s_1,\\
r_4 &: \quad s_1 + s_2 \xrightarrow{k_4} 2s_1 + s_2, & r_{11} &: \quad 2s_2 \xrightarrow{k_{11}} 3s_2,\\
r_5 &: \quad 3s_1 \xrightarrow{k_5} 4s_1, & r_{12} &: \quad 2s_1 + s_2 \xrightarrow{k_{12}} 2s_1 + 2s_2,\\
r_6 &: \quad 2s_1 + s_2 \xrightarrow{k_6} s_1 + s_2, & r_{13} &: \quad s_1 + 2s_2 \xrightarrow{k_{13}} s_1 + s_2,\\
r_7 &: \quad s_1 + 2s_2 \xrightarrow{k_7} 2s_2, & r_{14} &: \quad 3s_2 \xrightarrow{k_{14}} 2s_2, \qquad (3)
\end{aligned}$$

where $k_1, k_2, \ldots, k_{14}$ are the corresponding reaction rate coefficients. A par-

ticular choice of the (dimension-less) reaction coefficients is given by

$$\begin{aligned} k_1 &= 2 \times 10^{-7}, \quad k_2 = 19.9879, \quad k_3 = 0.0199, \quad k_4 = 0.02, \\ k_5 &= 2.9 \times 10^{-8}, \quad k_6 = 2.0002 \times 10^{-5}, \quad k_7 = 1.45 \times 10^{-8}, \\ k_8 &= 2 \times 10^{-7}, \quad k_9 = 8.3873, \quad k_{10} = 0.0384, \quad k_{11} = 0.0216, \\ k_{12} &= 2 \times 10^{-5}, \quad k_{13} = 1.571 \times 10^{-6}, \quad k_{14} = 10^{-5}, \end{aligned} \tag{4}$$

while the general conditions on these parameters are given later as equations (13) and (14).

In Figure 1, we display a representative noisy-time series generated using the Gillespie stochastic algorithm, in Figure 1(a) for the one-dimensional cubic Schlögl system [11], which deterministically displays two stable critical points (bistationarity [12]), in Figure 1(b) for the reaction network (1) with coefficients (2), which deterministically displays a stable critical point and a stable limit cycle (mixed bistability), and in Figure 1(c) for the reaction network (3) with coefficients (4), which deterministically displays two stable limit cycles (bicyclicity). Several statistical challenges arise. For example, is it possible to infer that the upper stable set in Figure 1(b) is a deterministic critical point, while the lower a noisy limit cycle? Is it possible to detect one/both noisy limit cycles in Figure 1(c)? The answer to the second question is complicated by the fact that the two deterministic limit cycles in Figure 1(c) are relatively close to each other.

The rest of the paper is organized as follows. In Section 2, we outline properties of the planar quadratic ODE systems, focusing on multistability, cycles and cycle bifurcations. There are two reasons for focusing on the planar quadratic systems: firstly, the phase plane theory for such systems is complete [13, 14], with a variety of concrete examples with interesting phase plane configurations [15, 16]. Secondly, an arbitrary planar quadratic ODE system can always be mapped to a kinetic one using only an affine transformation - a special property not shared with cubic (nor even linear) planar systems [17]. This, together with the available nonlinear kinetic transformations which increase the polynomial degree of an ODE system by one [2], imply that we may map a general planar quadratic system to at most cubic planar kinetic system, which may still be biologically or chemically relevant. In Section 3.2, we present the two planar cubic test models which induce reaction networks (1) and (3), and which are constructed starting from suitable planar quadratic ODE systems. We also briefly compare the deterministic and stochastic solutions of the two constructed systems.

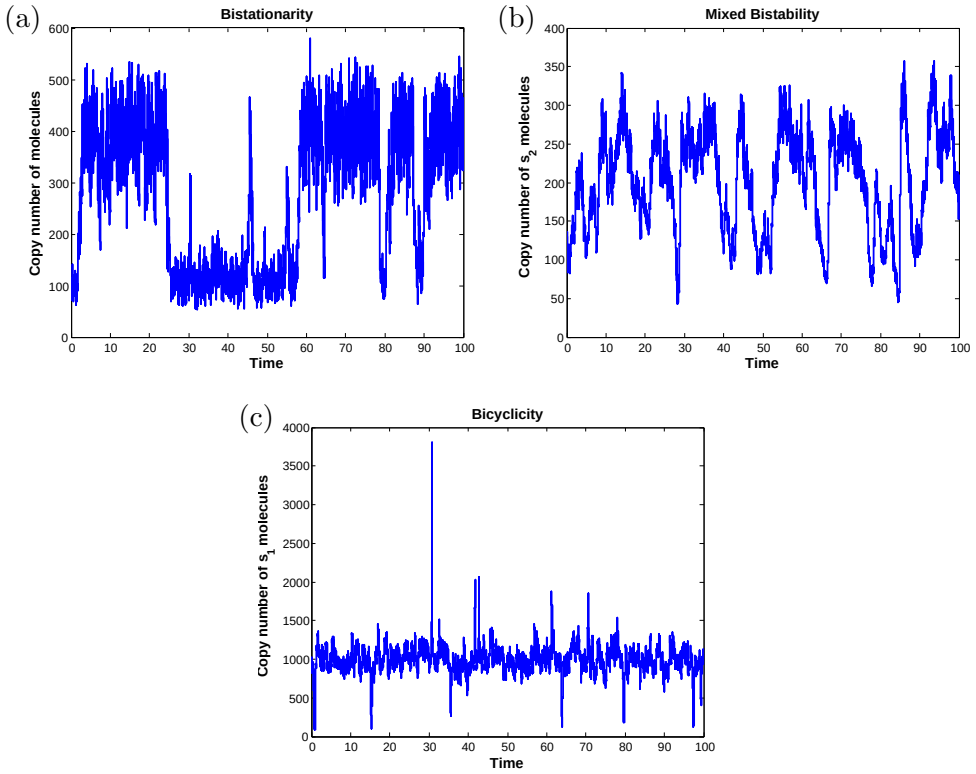

Figure 1: *Panels* (a), (b) *and* (c) *show representative sample paths generated using the Gillespie stochastic simulation algorithm for the Schlögl system* [11]*, reaction network* (1) *with coefficients* (2)*, and reaction network* (3) *with coefficients* (4)*, respectively. At the deterministic level, the phase planes of* (1) *and* (3) *are shown in Figure* 2*, while deterministic and stochastic time-series in Figures* 3 *and* 4*. At the deterministic level, a critical point and a limit cycle are 'hidden' in* (b)*, while two limit cycles are 'hidden' in* (c)*.*

2 Properties of two-dimensional second-degree polynomial ODEs: multistability, cycles and cycle bifurcations

Let us consider the two-dimensional second-degree autonomous polynomial ODEs

$$\begin{aligned}\frac{\mathrm{d}x_1}{\mathrm{d}t} &= \mathcal{P}_1(x_1, x_2; \mathbf{k}) = k_1 + k_2 x_1 + k_3 x_2 + k_4 x_1^2 + k_5 x_1 x_2 + k_6 x_2^2,\\ \frac{\mathrm{d}x_2}{\mathrm{d}t} &= \mathcal{P}_2(x_1, x_2; \mathbf{k}) = k_7 + k_8 x_1 + k_9 x_2 + k_{10} x_1^2 + k_{11} x_1 x_2 + k_{12} x_2^2, \quad (5)\end{aligned}$$

where $\mathcal{P}_i(\,\cdot\,,\,\cdot\,;\mathbf{k}) : \mathbb{R}^2 \to \mathbb{R}$, $i = 1, 2$, are the second-degree two-variable polynomial functions, and $\mathbf{k} = (k_1, k_2, \ldots, k_{12}) \in \mathbb{R}^{12}$ is the vector of the corresponding coefficients. We assume that $\mathcal{P}_1$ and $\mathcal{P}_2$ are relatively prime and at least one is of second-degree. We allow coefficients $\mathbf{k}$ to be parameter-dependent, $\mathbf{k} = \mathbf{k}(\mathbf{p})$, with $\mathbf{p} \in \mathbb{R}^q$, $q \geq 0$. Let us assume that system (5)

satisfies two additional properties:

(i) Coefficients k_1, k_3, k_6, k_7, k_8, $k_{10} \geq 0$, i.e. $\mathcal{P}_1$ and $\mathcal{P}_2$ are so-called kinetic functions (for a rigorous definition see [2]).

(ii) The species concentrations x_1 and x_2 are uniformly bounded in time for $t \geq 0$ in the nonnegative orthant $\mathbb{R}^2_{\geq}$, except possibly for initial conditions located on a finite number of one-dimensional subspaces of $\mathbb{R}^2_{\geq}$, where infinite-time blow-ups are allowed.

The subset of equations (5) satisfying properties (i)–(ii) are referred to as the *deterministic kinetic equations* bounded in $\mathbb{R}^2_{\geq}$, and denoted

$$\begin{aligned} \frac{\mathrm{d}x_1}{\mathrm{d}t} &= \mathcal{K}_1(x_1, x_2; \mathbf{k}(\mathbf{p})), \\ \frac{\mathrm{d}x_2}{\mathrm{d}t} &= \mathcal{K}_2(x_1, x_2; \mathbf{k}(\mathbf{p})). \end{aligned} \tag{6}$$

We now provide definitions and summarize a set of results regarding multistability, cycles and cycle bifurcations of (5) and (6), which are referred to as the so-called exotic phenomena in the biological context [12].

Multistability. System (5) is said to display multistability if multiple stable invariant sets coexist in the phase plane, for a fixed $\mathbf{k}$. Biologically, multistability corresponds to biological switches, which may be classified into reversible or irreversible [18, 19, 20], where the former play an important role in reversible biological processes (e.g. metabolic pathways dynamics, and reversible differentiation), while the latter in irreversible biological processes (e.g. developmental transitions, and apoptosis).

Multistability can be mathematically classified into *pure multistability*, involving stable invariant sets of only the same type (either only stable critical points, or only stable cycles), and *mixed multistability*, involving at least one stable critical point, and at least one stable cycle. Pure multistability involving only critical points is called *multistationarity* [12], while we call pure multistability involving only cycles *multicyclicity*. Mixed bistability, and bicyclicity, can be further classified into concentric and nonconcentric. Concentric mixed bistability (resp. bicyclicity) occurs when the stable limit cycle encloses the stable critical point (resp. when the first stable limit cycle encloses the second stable limit cycle), while nonconcentric when this is not the case.

We now prove that (5) can have at most three coexisting stable critical points, i.e. (5) can be at most *tristationary*. On the other hand, we conjecture that (6) can be maximally bistationary, and cannot display nonconcentric mixed bistability. Bistationarity has been shown to exist in (5) (even in one-dimensional cubic case, e.g. the Schlögl model [11], see the time-series shown in Figure 1(a)).

Lemma 2.1. *The maximum number of coexisting stable critical points in two-dimensional relatively prime second-degree polynomial ODE systems* (5)*, with fixed coefficients* **k***, is three.*

Proof. Let us assume system (5) has four, the maximum number, of real finite critical points. Then, using an appropriate centroaffine (linear) transformation [21, 22], system (5) can be mapped to

$$\begin{aligned}\frac{\mathrm{d}x_1}{\mathrm{d}t} &= a_1x_1(x_1-1)+b_1x_2(x_2-1)+c_1x_1x_2,\\ \frac{\mathrm{d}x_2}{\mathrm{d}t} &= a_2x_1(x_1-1)+b_2x_2(x_2-1)+c_2x_1x_2,\end{aligned} \tag{7}$$

which is topologically equivalent to (5), with the critical points located at $A=(0,0)$, $B=(1,0)$, $C=(0,1)$ and $D=(\alpha,\beta)$, with $\alpha\neq 0$, $\beta\neq 0$, $\alpha+\beta\neq 1$, and the coefficients c_1, c_2 given by

$$\begin{aligned}c_1 &= -\frac{\alpha-1}{\beta}a_1-\frac{\beta-1}{\alpha}b_1,\\ c_2 &= -\frac{\alpha-1}{\beta}a_2-\frac{\beta-1}{\alpha}b_2.\end{aligned}$$

The trace and determinant of the Jacobian matrix of (7), denoted τ and δ, respectively, evaluated at the four critical points, A, B, C, D, are given by:

$$\begin{aligned}
\tau_A &= -(a_1+b_2), & \delta_A &= a_1b_2-a_2b_1,\\
\tau_B &= a_1-a_2\frac{(\alpha-1)}{\beta}-b_2\frac{(\alpha+\beta-1)}{\alpha}, & \delta_B &= -\frac{\alpha+\beta-1}{\alpha}\delta_A,\\
\tau_C &= b_2-a_1\frac{(\alpha+\beta-1)}{\beta}-b_1\frac{(\beta-1)}{\alpha}, & \delta_C &= -\frac{\alpha+\beta-1}{\beta}\delta_A,\\
\tau_D &= \alpha a_1+\beta b_2-a_2\frac{\alpha(\alpha-1)}{\beta}-b_1\frac{\beta(\beta-1)}{\alpha}, & \delta_D &= (\alpha+\beta-1)\delta_A.
\end{aligned} \tag{8}$$

System (7) may have three stable critical points if and only if the quadrilateral $ABCD$, formed by the critical points, is nonconvex, and the only saddle critical point is the one located at the interior vertex of the quadrilateral [21, 22]. This is the case when $\alpha>0$, $\beta>0$, $\alpha+\beta<1$, and $\delta_A>0$, in which case A, B, and C are nonsaddle critical points, while D is a saddle. Imposing also the conditions $\tau_A<0$, $\tau_B<0$, $\tau_C<0$, ensuring that A, B, and C are stable, a solution of the resulting system of algebraic inequalities is given by $a_1=1$, $b_1=-1$, $a_2=1$, $0<\alpha<1/2\left((1+2\beta)-\sqrt{1+8\beta^2}\right)$, $-1<b_2<\alpha(-\alpha+\beta+1)/(\beta(\alpha+\beta-1))$. □

Let us note that if (7) is kinetic, then it cannot have three stable critical points. More precisely, requiring $b_1\geq 0$, $a_2\geq 0$, and $d_A>0$ and $\tau_A<0$

in (8), implies $a_1 > 0$ and $b_2 > 0$, which further implies $\tau_B > 0$, so that B is unstable.

Limit cycles. Cycles of (5) are closed orbits in the phase plane, and they can be isolated (limit cycles, and separatrix cycles) or nonisolated (a one-parameter continuous family of cycles). The separatrix cycles can be generally classified into the homoclinic cycles, heteroclinic cycles, and compound separatrix cycles, consisting of a finite union of separatrix cycles that are appropriately oriented [23]. Limit cycles correspond to biological clocks, which play an important role in fundamental biological processes, such as the cell cycle, the glycolytic cycle and circadian rhythms [24, 25, 26].

The maximum number of stable limit cycles in (5) is two, i.e. (5) can be at most *bicyclic*. This follows from the fact that the maximum number of limit cycles in (5) is four, in the unique configuration $(3, 1)$, a fact only recently proved in [14], solving the second part of Hilbert's 16th problem for the quadratic case. It also follows from [14] that (5) may display *mixed tristability*, involving one stable critical point, and two stable limit cycles. We conjecture that (6) has at most three limit cycles. Let us note that it was conjectured in [23], partially based on [27], that (5) bounded in the whole $\mathbb{R}^2$ can have at most two limit cycles.

Cycle bifurcations. Variations of coefficients $\mathbf{k}$ of (5) may lead to changes in the topology of the phase plane (e.g. a change may occur in the number of invariant sets or their stability, shape of their region of attraction or their relative position). The variation of $\mathbf{k}(\mathbf{p})$ in (6) may be interpreted as a variation of the reaction rate coefficients $\mathbf{k}$ due to changes in the reactor (environment) parameters $\mathbf{p}$, such as the pressure or temperature. If the variation causes the system to become topologically nonequivalent, such a parameter is called a bifurcation parameter, and at the parameter value where the topological nonequivalence occurs, a bifurcation is said to take place [28, 23]. Bifurcations in deterministic kinetic equations occur in applications [20, 24, 25, 26, 29, 10].

Bifurcations of cycles in the phase plane of (5) can be classified into three categories: (i) the Andronov-Hopf bifurcation, where a cycle is created from a critical point of focus or center type, (ii) the separatrix cycle bifurcation, where a limit cycle is created from a (compound) separatrix cycle, and (iii) the multiple limit cycle bifurcation, where a limit cycle is created from a limit cycle of multiplicity greater than one [13, 23]. Bifurcations (i) and (iii) are examples of local bifurcations, occurring in a neighbourhood of a critical point or a cycle, while bifurcations (ii) are examples of global bifurcations. Let us note that the maximum multiplicity of a multiple focus of (5) is three, so that at most three local limit cycles can be created under appropriate perturbations [30]. Convex homoclinic bifurcations (defined in e.g. [31]), as well as saddle-saddle bifurcations, and the saddle-node bifurcations on an invariant cycle, can occur in (5). However, concave homoclinic bifurcations, as well as double convex, and double concave homoclinic bifurcations [31],

cannot occur in (5) as a consequence of basic properties of planar quadratic ODEs [21, 22].

A necessary condition for the existence of a limit cycle in the phase plane of (6) is that $k_4 > 0$ or $k_{12} > 0$ [2]. This implies that the induced reaction network must contain at least one autocatalytic reaction with at least three products (i.e. three copy-numbers on the right-hand side of a reaction). Let us note that, for a fixed kinetic ODE system, multistationarity at some parameter values $\mathbf{k}$, is neither necessary, nor sufficient, for cycles at some (possibly other) parameter values $\mathbf{k}'$ [32]. In the literature, system (6) has been shown to display the following cycle bifurcations: Andronov-Hopf bifurcations, saddle-node on invariant cycle, and multiple limit cycle bifurcations leading to mixed bistability [17, 33, 34]. While reaction systems displaying double Andronov-Hopf bifurcation, a saddle-saddle heteroclinic bifucation, and displaying a multiple limit cycle bifurcation leading to concentric bicyclicity, have been constructed, the constructed systems are not bounded in $\mathbb{R}^2_{\geq}$ [17, 33, 34].

3 Test models: construction and simulations

In this section, we construct two planar cubic ODE systems displaying non-concentric bistability. The first system displays a convex homoclinic bifurcation, and mixed bistability, and is obtained by modifying the system from [2] using the results from Appendix A. The second system displays a multiple limit cycle bifurcation, and bicyclicity. To construct the second system, we use an existing system of the form (5), which forms a one-parameter family of uniformly rotated vector fields [36, 23], and which displays bicyclicity and multiple limit cycle bifurcation [35]. We use kinetic transformations from [2] to map this system, which is of the form (5), to a kinetic one, which is of the form (6), and we fine-tune the coefficients in such a way that the sizes of stable limit cycles differ by maximally one order of magnitude (a task that can pose challenges [15]). As differences may be observed between the deterministic and stochastic solutions for parameters at which a deterministic bifurcation occurs [5], we briefly investigate the constructed models for such observations. Let us note that an alternative static (i.e. not dynamic) approach for reaction system construction, using the chemical reaction network theory or kinetic logic, provides only conditions for stability of critical points, but no information about the phase plane structures [37], and is, thus, insufficient for construction of the systems presented in this paper.

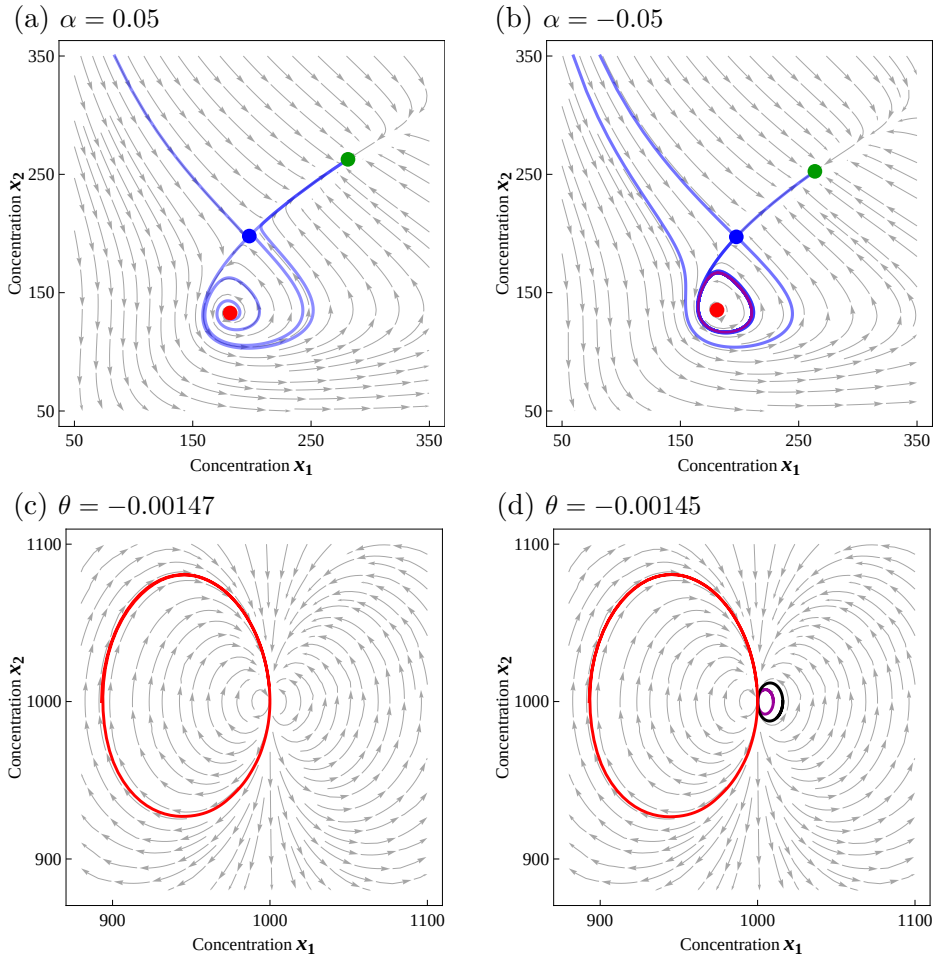

Figure 2: (a)–(b) *Phase plane diagrams of system* (9) *before and after the homoclinic bifurcation. The stable node, saddle, and unstable focus are represented as the green, blue and red dots, respectively, the vector field as gray arrows, numerically approximated saddle manifolds as blue trajectories, and the purple curve in panel* (b) *is the stable limit cycle. The parameters appearing in* (10)*, and satisfying* (11)*, are fixed to* $a = -0.8$, $\mathcal{T}_1 = \mathcal{T}_2 = 2$, $\varepsilon = 0.01$*, the reactor volume is set to* $V = 100$*, and the bifurcation parameter* α *is as shown in the panels.*
(c)–(d) *Phase plane diagrams of system* (12) *before and after the multiple limit cycle bifurcation. The stable limit cycles* L_1 *and* L_3 *are shown in red and purple, respectively, while the unstable limit cycle* L_2 *is shown in black. The parameters appearing in* (13)*, and satisfying* (14)*, are fixed to* $a = 1$, $b = -1$, $c = 0.5$, $d = 0.08$, $x_1^* = -3$, $\mathcal{T}_1 = \mathcal{T}_2 = 1000$, $\varepsilon = 0.01$*, the reactor volume is set to* $V = 1$*, and the bifurcation parameter* θ *is as shown in the panels.*

3.1 System 1: Homoclinic bifurcation and mixed bistability

Consider the following deterministic kinetic equations

$$\begin{aligned}\frac{\mathrm{d}x_1}{\mathrm{d}t} &= k_1 + k_2 x_1 + k_3 x_1^2 - k_4 x_1 x_2 - k_5 x_1^2 x_2 + k_6 x_1 x_2^2,\\ \frac{\mathrm{d}x_2}{\mathrm{d}t} &= k_7 - k_8 x_2 + k_9 x_1 x_2 + k_{10} x_2^2 - k_{11} x_2^3,\end{aligned} \tag{9}$$

with the coefficients $\mathbf{k} = \mathbf{k}(a, \boldsymbol{\mathcal{T}}, \alpha, \varepsilon)$ given by

$$\begin{aligned}
k_1 &= \varepsilon, & k_7 &= \varepsilon,\\
k_2 &= \frac{1}{2}\left|\left(3\left(\mathcal{T}_2 - \frac{2}{3}\right)(a\mathcal{T}_1 + \mathcal{T}_2) - 2\alpha\mathcal{T}_1\right)\right|, & k_8 &= |-\mathcal{T}_1 + a\mathcal{T}_2(\mathcal{T}_2 - 1)|,\\
k_3 &= \left|-\frac{3}{2}a\left(\mathcal{T}_2 - \frac{2}{3}\right) + \alpha\right|, & k_9 &= 1,\\
k_4 &= \left|1 - \frac{3}{2}(a\mathcal{T}_1 + 2\mathcal{T}_2)\right|, & k_{10} &= \left|2a\left(\mathcal{T}_2 - \frac{1}{2}\right)\right|,\\
k_5 &= \left|\frac{3}{2}a\right|, & k_{11} &= |a|,\\
k_6 &= \frac{3}{2}, &&
\end{aligned} \tag{10}$$

where $|\cdot|$ denotes the absolute value, and with parameters a, α, ε, $\mathcal{T}_1$, and $\mathcal{T}_2$ satisfying

$$\begin{aligned}
&a \in (-1, 0), \quad |\alpha| \ll 1, \quad 1 \ll \varepsilon \leq 0,\\
&\mathcal{T}_1 > \frac{2\sqrt{3}}{9}, \quad \mathcal{T}_2 \in \left(\max(1, -a\mathcal{T}_1), \frac{2}{3} + \frac{8}{3}a^{-2}(3 - a^2)(a + 4\mathcal{T}_1)\right).
\end{aligned} \tag{11}$$

The canonical reaction network [2] induced by system (9) is given by (1).

System (9) is obtained from system [2, eq. (32)], which is known to display a mixed bistability and a convex supercritical homoclinic bifurcation when $\alpha = 0, \varepsilon = 0$. We have modified [2, eq. (32)] by adding to its right-hand side the ε-term from Definition A.1, thus preventing the long-term dynamics to be trapped on the phase plane axes. It can be shown, using Theorem A.1, that choosing a sufficiently small $\varepsilon > 0$ in (10) does not introduce additional critical points in first quadrant of the phase space of (9).

In Figures 2(a) and 2(b), we show phase plane diagrams of (9) before and after the bifurcation, respectively, where the critical points of the system are shown as the coloured dots (the stable node, saddle, and unstable focus are shown as the green, blue and red dots, respectively), the blue curves are numerically approximated saddle manifolds (which at $\alpha = 0$, $\varepsilon = 0$ form a homoclinic loop [2]), and the purple curve in Figure 2(b) is the stable limit cycle that is created from the homoclinic loop. Let us note that the

parameter α, appearing in (10), controls the bifurcation, while the parameter a controls the saddle-node separation [2].

In Figure 3, we show numerical solutions of the initial value problem for (9) in red, with one initial condition in the region of attraction of the node, while the other near the unstable focus. The blue sample paths are generated by using the Gillespie stochastic simulation algorithm on the induced reaction network (1), initiated near the unstable focus. More precisely, in Figures 3(a) and 3(c) we show the dynamics before the deterministic bifurcation, when the node is the globally stable critical point for the deterministic model, while in Figures 3(b) and 3(d) we show the dynamics after the bifurcation, when the deterministic model displays mixed bistability. On the other hand, the stochastic model displays relatively frequent stochastic switching in Figures 3(a) and 3(b), when the saddle-node separation is relatively small. Let us emphasize that the stochastic switching is observed even before the deterministic bifurcation. In Figures 3(c) and 3(d), when the saddle-node separation is relatively large, the stochastic switching is less common, and the stochastic system in the phase space is more likely located near the stable node. Thus, in Figures 3(c) and 3(d), the stochastic system is less affected by the bifurcation than the deterministic system, and, in fact, behaves more like the deterministic system before the bifurcation.

In [38], an algorithm is presented which structurally modifies a given reaction network under the mass-action kinetics, in such a way that the deterministic dynamics is preserved, while the stochastic dynamics is modified in a state-dependent manner. Applying the algorithm on the reaction network (1), we preserve the deterministic kinetic equations (9), while decreasing the chance of finding the stochastic state near the stable node in Figures 3(c) and 3(d), and restoring the stochastic switching.

3.2 System 2: Multiple limit cycle bifurcation and bicyclicity

Consider the following deterministic kinetic equations

$$\begin{aligned}\frac{\mathrm{d}x_1}{\mathrm{d}t} &= k_1 + x_1(k_2 + k_3x_1 + k_4x_2 + k_5x_1^2 + k_6x_1x_2 + k_7x_2^2),\\ \frac{\mathrm{d}x_2}{\mathrm{d}t} &= k_8 + x_2(k_9 + k_{10}x_1 + k_{11}x_2 + k_{12}x_1^2 + k_{13}x_1x_2 + k_{14}x_2^2),\end{aligned} \tag{12}$$

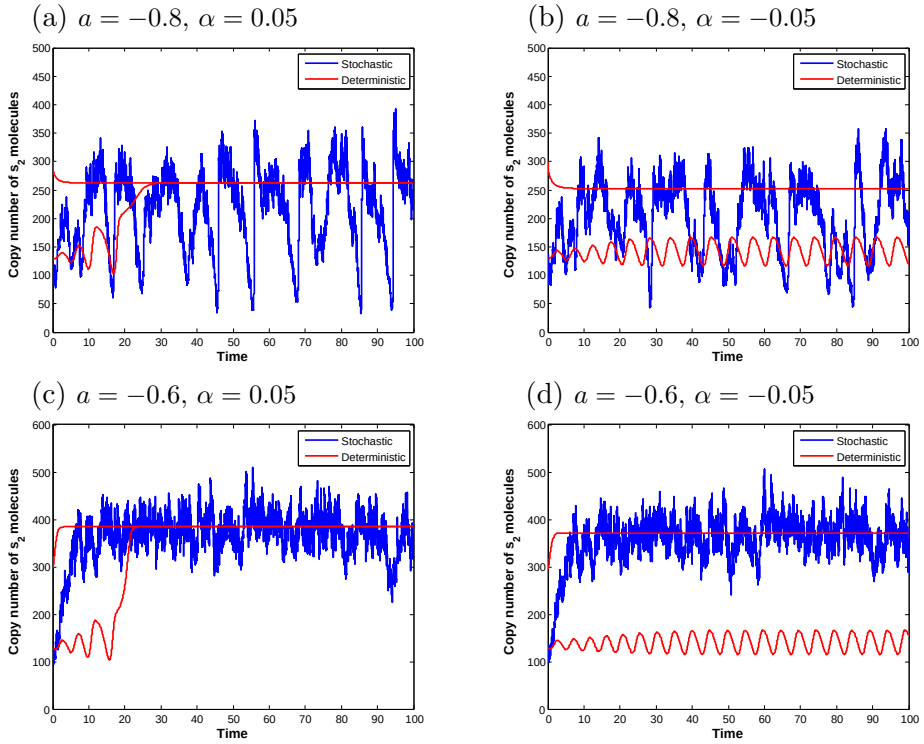

Figure 3: *Numerical solutions of system* (9) *are shown in red, while representative sample paths generated by the Gillespie stochastic simulation algorithm applied on the corresponding reaction network* (1) *are shown in blue.*
(a)–(b) *The cases before and after the homoclinic bifurcation, respectively, for smaller values of* a*, when the limit cycle and the stable node are closer together.*
(c)–(d) *The cases before and after the homoclinic bifurcation, respectively, for larger values of* a*.*
One of the deterministic solutions is initiated in the region of attraction of the node, while the other near the focus. The parameters are fixed to $\mathcal{T}_1 = \mathcal{T}_2 = 2$*,* $\varepsilon = 0.01$*, the reactor volume is set to* $V = 100$*, with* a *and* α *as shown in the panels.*

with coefficients $\mathbf{k} = \mathbf{k}(a, b, c, d, x_1^*, \boldsymbol{\mathcal{T}}, \theta, \varepsilon)$ given by

$$
\begin{aligned}
k_1 &= k_8 = \varepsilon, \\
k_2 &= |-a\mathcal{T}_1\mathcal{T}_2\cos(\theta) + [(d(\mathcal{T}_1+1) + c\mathcal{T}_2)\mathcal{T}_2 + b(\mathcal{T}_1+1)(\mathcal{T}_1+x_1^*)]\sin(\theta)|, \\
k_3 &= |a\mathcal{T}_2\cos(\theta) - [d\mathcal{T}_2 + b(2\mathcal{T}_1 + x_1^* + 1)]\sin(\theta)|, \\
k_4 &= |a\mathcal{T}_1\cos(\theta) - [d(\mathcal{T}_1+1) + 2c\mathcal{T}_2]\sin(\theta)|, \\
k_5 &= |b\sin(\theta)|, \\
k_6 &= |-a\cos(\theta) + d\sin(\theta)|, \\
k_7 &= |c\sin(\theta)|,
\end{aligned}
\tag{13}
$$

and if $k_i = |f(a, b, c, d, x_1^*, \boldsymbol{\mathcal{T}})\cos(\theta) - g(a, b, c, d, x_1^*, \boldsymbol{\mathcal{T}})\sin(\theta)|$, then $k_{i+7} = |f(a, b, c, d, x_1^*, \boldsymbol{\mathcal{T}})\sin(\theta) + g(a, b, c, d, x_1^*, \boldsymbol{\mathcal{T}})\cos(\theta)|$, $i = 2, 3, \ldots, 7$, and with

parameters a, b, c, d, x_1^*, $\mathcal{T}_1$, $\mathcal{T}_2$, θ and ε satisfying

$$\begin{aligned} 0 \leq \varepsilon \ll 1, \quad -1 \ll \theta < 0, \\ b < 0, \quad d > 0, \quad a > -\frac{d^2}{4b}, \quad 0 < c < a + \frac{d^2}{4b}, \quad x_1^* < \frac{d^2}{4bc}, \\ a^3 c + b^3 (1 - x_1^*)^2 \neq 0, \\ \mathcal{T}_1 > -x_1^*, \quad 0 < \mathcal{T}_2 < -\frac{4abx_1^*}{d^2(x_0 - 1)}(\mathcal{T}_1 + x_1^*), \\ [d(\mathcal{T}_1 + 1) + c\mathcal{T}_2]\mathcal{T}_2 + b(\mathcal{T}_1 + 1)(\mathcal{T}_1 + x_1^*) < 0. \end{aligned} \tag{14}$$

The canonical reaction network induced by system (12) is given by (3). In this section, we show that systems (12) and (15) (see below), the latter of which is known to display bicyclicity and a multiple limit cycle bifurcation, are topologically equivalent near the corresponding critical points, provided conditions (14) are satisfied.

In Figures 2(c) and 2(d), we show the phase plane diagram of (12) for a particular choice of the parameters satisfying (14), and it can be seen that the system also displays bicyclicity and a multiple limit cycle bifurcation, with Figures 2(c) and 2(d) showing the cases before and after the bifurcation, respectively. In Figure 2(c), the only stable invariant set is the limit cycle shown in red, while in Figure 2(d) there are two additional limit cycles - a stable one, shown in purple, and an unstable one, shown in black. The black, purple, and red limit cycles are denoted in the rest of the paper by L_1, L_2 and L_3, respectively. At the bifurcation point, L_1 and L_2 intersect.

In order to construct (12), let us consider the planar quadratic ODE system [35, 17] given by

$$\begin{aligned} \frac{\mathrm{d}x_1}{\mathrm{d}t} &= \mathcal{Q}_1(x_1, x_2)\cos(\theta) - \mathcal{Q}_2(x_1, x_2)\sin(\theta), \\ \frac{\mathrm{d}x_2}{\mathrm{d}t} &= \mathcal{Q}_1(x_1, x_2)\sin(\theta) + \mathcal{Q}_2(x_1, x_2)\cos(\theta), \end{aligned} \tag{15}$$

where

$$\begin{aligned} \mathcal{Q}_1(x_1, x_2) &= -ax_1x_2, \\ \mathcal{Q}_2(x_1, x_2) &= -bx_1^* + b(x_1^* + 1)x_1 + dx_2 - bx_1^2 - dx_1x_2 - cx_2^2, \end{aligned} \tag{16}$$

with

$$\begin{aligned} x_1^* < 0, \ d^2 - 4bcx_1^* < 0, \ d^2 - 4b(c - a) < 0, \\ \theta d\,(a - b(1 - x_1^*)) < 0, \ \ \theta bd > 0, \ \ a^3 c + b^3(1 - x_1^*)^2 \neq 0. \end{aligned} \tag{17}$$

Lemma 3.1. *Consider system* (15)–(17)*, with the real parameter* $\theta \in (-\pi, \pi]$*. Function* $\boldsymbol{\mathcal{P}}(x_1, x_2; \theta) = (\mathcal{Q}_1\cos(\theta) - \mathcal{Q}_2\sin(\theta), \mathcal{Q}_1\sin(\theta) + \mathcal{Q}_2\cos(\theta))$ *forms a* one-parameter family of uniformly rotated vector fields *with the rotation parameter* θ*, and the following results hold:*

1. Finite critical points. *System* (15) *has two critical points in the finite part of the phase plane, located at* $(1,0)$ *and* $(x_1^*,0)$*, both of which are unstable foci when* $|\theta| \ll 1$*.*

2. Number and distribution of limit cycles. *System* (15) *has three limit cycles in the configuration* $(2,1)$ *when* $|\theta| \ll 1$*. The focus located at* $(1,0)$ *is surrounded by two positively oriented limit cycles* L_1 *and* L_2*, with the unstable limit cycle* L_2 *enclosing the stable limit cycle* L_1*, while the focus at* $(x_1^*,0)$ *by a single negatively oriented stable limit cycle* L_3*.*

3. Dependence of the limit cycles on the rotation parameter θ*. There exists a critical value* $\theta = \theta^* < 0$*, at which the limit cycles* L_1 *and* L_2 *intersect in a semistable, positively oriented limit cycle that is stable from the inside, and unstable from the outside. As* θ *is monotonically increased in* $(\theta^*,0)$*, the limit cycles* L_2 *and* L_3 *monotonically expand, while* L_1 *monotonically contracts.*

Proof. The statement of the lemma follows from [35, 17], and the theory of one-parameter family of uniformly rotated vector fields [36, 23]. □

In order to map the stable limit cycles of system (15) into the first quadrant, and then map the resulting system to a kinetic one, having no boundary critical points, let us apply a translation transformation $\Psi_{\mathcal{T}}$ [2], $\boldsymbol{\mathcal{T}} = (\mathcal{T}_1, \mathcal{T}_2) \in \mathbb{R}^2$, followed by a perturbed x-factorable transformation, as defined in Definition A.1, on system (15), which results in system (12) with the coefficients (13).

Theorem 3.1. *Consider the ODE systems* (12) *and* (15)*, and assume conditions* (14) *are satisfied. Then* (12) *and* (15) *are locally topologically equivalent in the neighborhood of the corresponding critical points. Furthermore, for sufficiently small* $\varepsilon > 0$*, system* (12) *has exactly one additional critical point in* $\mathbb{R}^2_>$*, which is a saddle located in the neigbhourhood of* $(\mathcal{T}_1, 0)$*.*

Proof. Consider the critical point $(1,0)$ of system (15), which corresponds to the critical point $(\mathcal{T}_1 + 1, \mathcal{T}_2)$ of system (12) when $\varepsilon = 0$. The Jacobian matrices of (15), and (12) with $\varepsilon = 0$, evaluated at $(1,0)$, and $(\mathcal{T}_1 + 1, \mathcal{T}_2)$, are respectively given by

$$J = \begin{pmatrix} -b(x_1^* - 1)\sin(\theta) & -a\cos(\theta) \\ b(x_1^* - 1)\cos(\theta) & -a\sin(\theta) \end{pmatrix},$$

$$J_{\mathcal{X},\mathcal{T}} = \begin{pmatrix} -b(x_1^* - 1)(\mathcal{T}_1 + 1)\sin(\theta) & -a(\mathcal{T}_1 + 1)\cos(\theta) \\ b(x_1^* - 1)\mathcal{T}_2\cos(\theta) & -a\mathcal{T}_2\sin(\theta) \end{pmatrix}.$$

Condition (ii) of [2, Theorem 3.3] is satisfied, so that the stability of the critical point is preserved under the x-factorable transformation, but condition (iii) is not satisfied. In order for $(\mathcal{T}_1 + 1, \mathcal{T}_2)$ to remain focus under the

x-factorable transformation, the discriminant of $J_{\mathcal{X},\mathcal{T}}$ must be negative:

$$(a\mathcal{T}_2 + b(\mathcal{T}_1+1)(x_1^*-1))^2(\sin(\theta))^2 - 4ab(x_1^*-1)(\mathcal{T}_1+1)\mathcal{T}_2 < 0. \qquad (18)$$

Let us set $\theta = 0$ in (18), leading to

$$-4ab(x_1^*-1)(\mathcal{T}_1+1)\mathcal{T}_2 < 0. \qquad (19)$$

Conditions (18) and (19) are equivalent when $|\theta| \ll 1$, since the the sign of the function on the LHS of (18) is a continuous function of θ. From conditions (14) it follows that $ab < 0$, $x_1^* < 0$, and $\mathcal{T}_1, \mathcal{T}_2 > 0$, so that (19) is satisfied. Similar arguments show that the second critical point of (15), located at $(x_1^*, 0)$, is mapped to an unstable focus of (12), if $d > 0$, and if $\mathcal{T}_2$ is bounded as given in (14).

Consider (12) with $\varepsilon = 0$. The boundary critical points are located at $(0,0)$, $(\mathcal{T}_1, 0)$, and $(0, x_{2,\pm}^*)$, with

$$x_{2,\pm}^* = \frac{1}{2c}\left(d(\mathcal{T}_1+1) + 2c\mathcal{T}_2 \pm \sqrt{(\mathcal{T}_1+1)(d^2(\mathcal{T}_1+1) - 4bc(\mathcal{T}_1+x_1^*))}\right).$$

Conditions (14) imply that the critical point $(0,0)$ satisfies $\mathcal{P}_1(0,0) = -a\mathcal{T}_1\mathcal{T}_2 < 0$, and

$$\mathcal{P}_2(0,0) = -[d(1+\mathcal{T}_1) + c\mathcal{T}_2]\mathcal{T}_2 - b(1+\mathcal{T}_1)(\mathcal{T}_1 + x_1^*) > 0,$$

when $\theta = 0$. When $|\theta| \ll 1$, it then follows from condition (iv) of [2, Theorem 3.3] that the critical point is a saddle, and from Theorem A.1, condition (23), that it is mapped outside of $\mathbb{R}^2_{\geq}$ when $\varepsilon \neq 0$. Similar arguments show that, assuming conditions (14) are true, $(\mathcal{T}_1, 0)$ is a saddle that is mapped to $\mathbb{R}^2_{>}$ when $\varepsilon \neq 0$, and that critical points $(0, x_{2,\pm}^*)$ are real, $x_{2,-}^* < 0$, and that $(0, x_{2,+}^*)$ is a saddle that is mapped outside $\mathbb{R}^2_{\geq}$ when $\varepsilon \neq 0$.

Finally, if conditions (14) are satisfied, so are conditions (17). □

We now consider the kinetic ODEs (12) and the induced reaction network (4) for a particular set of coefficients (13). We also rescale the time according to $t \to 2 \times 10^{-5}\, t$, i.e. we multiply all the coefficients $k_1, \ldots k_{14}$ appearing in (12) by 2×10^{-5}. In Figures 4(a) and 4(b) we show the numerically approximated solutions of the initial value problem for (12) before and after the bifurcation, respectively. In Figure 4(a), the solution is initiated near the unstable focus outside the limit cycle L_3, and it can be seen that the solution spends some time near the unstable focus, followed by an excursion that leads it to the stable limit cycle L_3, where is then stays forever. In Figure 4(b), the solutions tend to the limit cycle L_1 or L_3, depending on the initial condition. Let us note that the critical value at which the limit cycles L_1 and L_2 intersect, at the deterministic level, is numerically found to be $\theta^* \approx -0.00146$. In Figures 4(c) and 4(d) we show representative sample

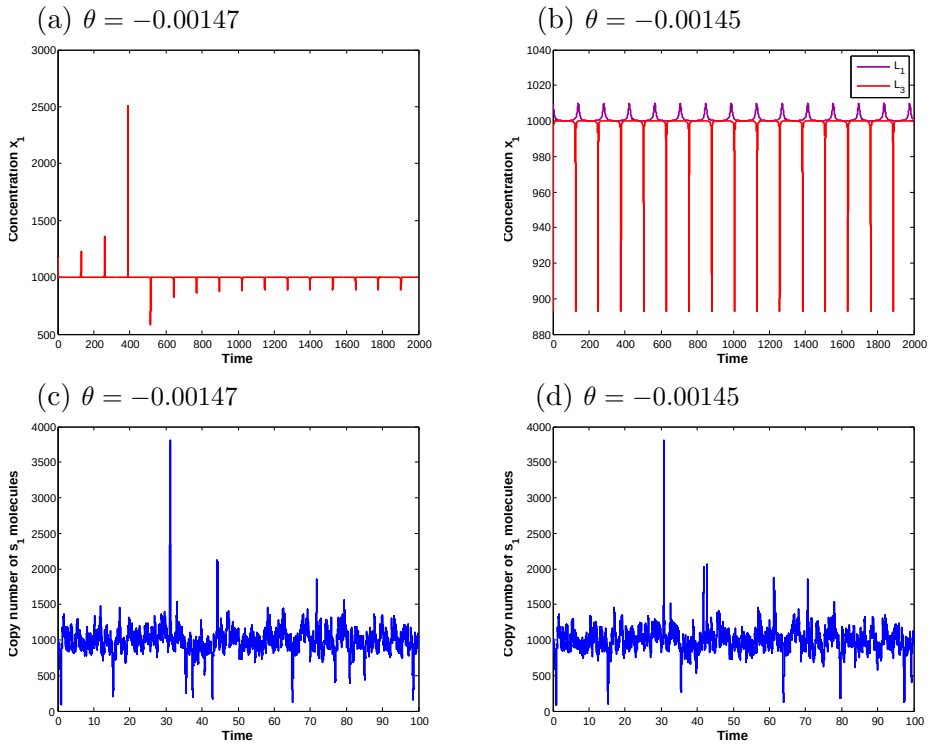

Figure 4: (a)–(b) *Numerical solutions of the kinetic ODE system given by* (12) *before and after the bifurcation, where in* (b) *the trajectory initiated near the stable limit cycle* L_1 *is shown in purple, while the on initiated near* L_3 *in red.*
(c)–(d) *Sample paths generated by the Gillespie stochastic simulation algorithm applied to the induced reaction network* (3) *before and after the bifuration.*
The parameters appearing in (13) *are fixed to* $a = 1$, $b = -1$, $c = 0.5$, $d = 0.08$, $x_1^* = -3$, $\mathcal{T}_1 = \mathcal{T}_2 = 1000$, $\varepsilon = 0.01$, *with the reactor volume* $V = 1$, *and* θ *as indicated in the plots. Coefficients* (13) *are multiplied by a constant factor of* 2×10^{-5} *(time-rescaling).*

paths generated by applying the Gillespie stochastic simulation algorithm on the reaction network (3), before and after the bifurcation, respectively. One can notice that the stochastic dynamics does not appear to be significantly influenced by the bifurcation, as opposed to the deterministic dynamics. In Figure 4(d), one can notice pulses similar to those seen in plot Figure 4(c), that are now induced by the intrinsic noise present in the system.

Acknowledgments: The authors would like to thank the Isaac Newton Institute for Mathematical Sciences, Cambridge, for support and hospitality during the programme "Stochastic Dynamical Systems in Biology: Numerical Methods and Applications" where work on this paper was undertaken. This work was supported by EPSRC grant no EP/K032208/1. This work was partially supported by a grant from the Simons Foundation. Tomáš Vejchodský would like to acknowledge the institutional support RVO 67985840. Radek Erban would also like to thank the Royal Society for a University Research Fellowship.

Appendix A: Perturbed X-factorable transformation

Definition A.1. Consider applying an x-factorable transformation, as defined in [2], on (5), and then adding to the resulting right-hand side a zero-degree term $\varepsilon\mathbf{v}$, with $\varepsilon \geq 0$ and vector $\mathbf{v} = (1,1)^\top$, resulting in

$$\frac{\mathrm{d}\mathbf{x}}{\mathrm{d}t} = \varepsilon\mathbf{v} + \mathcal{X}(\mathbf{x})\boldsymbol{\mathcal{P}}(\mathbf{x};\,\mathbf{k}) \;=\; \varepsilon\mathbf{v} + (\Psi_{\mathcal{X}}\boldsymbol{\mathcal{P}})(\mathbf{x};\,\mathbf{k}) \equiv (\Psi_{\mathcal{X}_\varepsilon}\boldsymbol{\mathcal{P}})(\mathbf{x};\,\mathbf{k}). \tag{20}$$

Then $\Psi_{\mathcal{X}_\varepsilon} : \mathbb{P}_2(\mathbb{R}^2;\,\mathbb{R}^2) \to \mathbb{P}_3(\mathbb{R}^2;\,\mathbb{R}^2)$, mapping $\boldsymbol{\mathcal{P}}(\mathbf{x};\,\mathbf{k})$ to $(\Psi_{\mathcal{X}_\varepsilon}\boldsymbol{\mathcal{P}})(\mathbf{x};\,\mathbf{k})$, is called a *perturbed x-factorable transformation* if $\varepsilon \neq 0$. If $\varepsilon = 0$, the transformation reduces to an (unperturbed) x-factorable transformation, $\Psi_{\mathcal{X}} \equiv \Psi_{\mathcal{X}_0}$, defined in [2].

Lemma A.1. $(\Psi_{\mathcal{X}_\varepsilon}\boldsymbol{\mathcal{P}})(\mathbf{x};\,\mathbf{k})$ from *Defnition* A.1 is a *kinetic function*, i.e. $(\Psi_{\mathcal{X}_\varepsilon}\boldsymbol{\mathcal{P}})(\mathbf{x};\,\mathbf{k}) \in \mathbb{P}_3^{\mathcal{K}}(\mathbb{R}^2_{\geq};\,\mathbb{R}^2)$.

Proof. $(\Psi_{\mathcal{X}}\boldsymbol{\mathcal{P}})(\mathbf{x};\,\mathbf{k})$ is a kinetic function [2]. Since, from (20), $(\Psi_{\mathcal{X}_\varepsilon}\boldsymbol{\mathcal{P}})(\mathbf{x};\,\mathbf{k}) = \varepsilon\mathbf{v} + (\Psi_{\mathcal{X}}\boldsymbol{\mathcal{P}})(\mathbf{x};\,\mathbf{k})$, with $\varepsilon \geq 0$ and $\mathbf{v} = (1,1)^\top$, it follows that $(\Psi_{\mathcal{X}_\varepsilon}\boldsymbol{\mathcal{P}})(\mathbf{x};\,\mathbf{k})$ is kinetic as well. □

We now provide a theorem relating location, stability and type of the positive critical points of (5) and (20).

Theorem A.1. *Consider the ODE system* (5) *with positive critical points* $\mathbf{x}^* \in \mathbb{R}^2_{>}$. *Let us assume that* $\mathbf{x}^* \in \mathbb{R}^2_{>}$ *is hyperbolic, and is not the degenerate case between a node and a focus, i.e. it satisfies the condition*

$$\left(\mathrm{tr}\left(\nabla\boldsymbol{\mathcal{P}}(\mathbf{x}^*;\,\mathbf{k})\right)\right)^2 - 4\det\left(\nabla\boldsymbol{\mathcal{P}}(\mathbf{x}^*;\,\mathbf{k})\right) \neq 0, \tag{21}$$

as well as conditions (ii) *and* (iii) *of* Theorem 3.3 *in* [2]. *Then positivity, stability and type of the critical point* $\mathbf{x}^* \in \mathbb{R}^2_{>}$ *are invariant under the perturbed x-factorable transformations* $\Psi_{\mathcal{X}_\varepsilon}$, *for sufficiently small* $\varepsilon \geq 0$. *Assume* (5) *does not have boundary critical points. Consider the two-dimensional ODE system* (20) *with* $\varepsilon = 0$, *and with boundary critical points denoted* $\bar{\mathbf{x}}^0 \in \mathbb{R}^2_{\geq}$, $\bar{\mathbf{x}}^0 = (\bar{x}^0_{b,1}, \bar{x}^0_{b,2})$, $\bar{x}^0_{b,1}\bar{x}^0_{b,2} = 0$. *Assume that for* $i \in \{1,2\}$

$$\frac{\partial\mathcal{P}_i(\bar{\mathbf{x}}^0_b;\,\mathbf{k})}{\partial x_i} \neq 0, \qquad \textit{if} \;\; \bar{x}^0_{b,i} \neq 0, \tag{22}$$

and that for some $i \in \{1,2\}$

$$\mathcal{P}_i(\bar{\mathbf{x}}^0_b;\,\mathbf{k}) > 0, \qquad \textit{if} \;\; \bar{x}^0_{b,i} = 0. \tag{23}$$

Then, the critical point $\bar{\mathbf{x}}^0_b \in \mathbb{R}^2_{\geq}$ *of the two-dimensional ODE system* (20) *with* $\varepsilon = 0$ *becomes the critical point* $\bar{\mathbf{x}}_b \notin \mathbb{R}^2_{\geq}$ *of system* (20) *for sufficiently small* $\varepsilon > 0$.

Proof. The critical points of (20) are solutions of the following regularly perturbed algebraic equation

$$\varepsilon \mathbf{v} + \mathcal{X}(\bar{\mathbf{x}})\boldsymbol{\mathcal{P}}(\bar{\mathbf{x}};\, \mathbf{k}) = \mathbf{0}. \tag{24}$$

Let us assume $\bar{\mathbf{x}}$ can be written as the power series

$$\bar{\mathbf{x}} = \bar{\mathbf{x}}^0 + \varepsilon \bar{\mathbf{x}}^1 + \mathcal{O}(\varepsilon^2), \tag{25}$$

where $\bar{\mathbf{x}}^0 \in \mathbb{R}^2_{\geq}$ are the critical points of (20) with $\varepsilon = 0$. Substituting the power series (25) into (24), and using the Taylor series theorem on $\boldsymbol{\mathcal{P}}(\bar{\mathbf{x}};\, \mathbf{k})$, so that $\boldsymbol{\mathcal{P}}(\bar{\mathbf{x}}^0 + \varepsilon\bar{\mathbf{x}}^1 + \mathcal{O}(\varepsilon^2);\, \mathbf{k}) = \boldsymbol{\mathcal{P}}(\bar{\mathbf{x}}^0;\, \mathbf{k}) + \varepsilon\nabla\boldsymbol{\mathcal{P}}(\bar{\mathbf{x}}^0;\, \mathbf{k})\bar{\mathbf{x}}^1 + \mathcal{O}(\varepsilon^2)$, as well as that $\mathcal{X}(\bar{\mathbf{x}}) = \mathcal{X}(\bar{\mathbf{x}}^0) + \varepsilon\mathcal{X}(\bar{\mathbf{x}}^1) + \mathcal{O}(\varepsilon^2)$, and equating terms of equal powers in ε, the following system of polynomial equations is obtained:

$$\begin{aligned} \mathcal{O}(1) &: \mathcal{X}(\bar{\mathbf{x}}^0)\boldsymbol{\mathcal{P}}(\bar{\mathbf{x}}^0;\, \mathbf{k}) = 0, \\ \mathcal{O}(\varepsilon) &: \mathcal{X}(\bar{\mathbf{x}}^0)\nabla\boldsymbol{\mathcal{P}}(\bar{\mathbf{x}}^0;\, \mathbf{k})\bar{\mathbf{x}}^1 + \mathcal{X}(\bar{\mathbf{x}}^1)\boldsymbol{\mathcal{P}}(\bar{\mathbf{x}}^0;\, \mathbf{k}) = -\mathbf{v}. \end{aligned} \tag{26}$$

Order 1 *equation.* The positive critical points $\bar{\mathbf{x}}^0 \in \mathbb{R}^S_{>}$ satisfy $\boldsymbol{\mathcal{P}}(\bar{\mathbf{x}}^0;\, \mathbf{k}) = \mathbf{0}$. Since $\boldsymbol{\mathcal{P}}(\mathbf{x};\, \mathbf{k})$ has no boundary critical points by assumption, critical points $\bar{\mathbf{x}}^0_b \in \mathbb{R}^S_{\geq}$ with $\bar{x}^0_{b,i} = 0$, $\bar{x}^0_{b,j} \neq 0$, $\bar{x}^0_{b,1}\bar{x}^0_{b,2} = 0$, $i, j \in \{1, 2\}$, satisfy $\mathcal{P}_i(\bar{\mathbf{x}}^0_b;\, \mathbf{k}) \neq 0$, $\mathcal{P}_j(\bar{\mathbf{x}}^0_b;\, \mathbf{k}) = 0$.

Order ε *equation.* Vector $\bar{\mathbf{x}}^1$ satisfies system

$$\mathcal{X}(\bar{\mathbf{x}}^0)\nabla\boldsymbol{\mathcal{P}}(\bar{\mathbf{x}}^0;\, \mathbf{k})\bar{\mathbf{x}}^1 = -\mathbf{v},$$

which can be solved provided $\bar{\mathbf{x}}^0$ is a hyperbolic critical point. Vector $\bar{\mathbf{x}}^1_b$ is given by

$$\bar{x}^1_{b,i} = \begin{cases} -(\mathcal{P}_i(\bar{\mathbf{x}}^0_b;\, \mathbf{k}))^{-1}, & \text{if } \bar{x}^0_{b,i} = 0, \\ (\frac{\partial \mathcal{P}_i(\bar{\mathbf{x}}^0_b;\mathbf{k})}{\partial x_i})^{-1}\left((\mathcal{P}_j(\bar{\mathbf{x}}^0_b;\, \mathbf{k}))^{-1}\frac{\partial \mathcal{P}_i(\bar{\mathbf{x}}^0_b;\mathbf{k})}{\partial x_j} - (\bar{x}^0_{b,i})^{-1}\right), & \text{if } \bar{x}^0_{b,i} \neq 0, \end{cases}$$

from which conditions (22) and (23) follow. □

References

[1] Pineda-Krch, M., Blok, H. J., Dieckmann, U., Doebeli, M., 2007. A tale of two cycles – distinguishing quasi-cycles and limit cycles in finite predator-prey populations. *Oikos*, **116**(**1**): 53–64.

[2] Plesa, T., Vejchodský, T., and Erban, R., 2015. Chemical Reaction Systems with a Homoclinic Bifurcation: An Inverse Problem. Submitted to *Journal of Mathematical Chemistry*, available as http://arxiv.org/abs/1510.07205.

[3] Toner, D. L. K., Grima R., 2013. Molecular noise induces concentration oscillations in chemical systems with stable node steady states. *The Journal of Chemical Physics*, **138**, 055101.

[4] Louca, S., Doebeli, M., 2014. Distinguishing intrinsic limit cycles from forced oscillations in ecological time series. *Theoretical Ecology*, **7**(**4**): 381–390.

[5] Erban, R., Chapman, S. J., Kevrekidis, I. and Vejchodský, T., 2009. Analysis of a stochastic chemical system close to a SNIPER bifurcation of its mean-field model. *SIAM Journal on Applied Mathematics*, **70**(**3**): 984–1016.

[6] Thomas, P., Straube, A. V., Timmer, J., Fleck, C., Grima R., 2013. Signatures of nonlinearity in single cell noise-induced oscillations. *Journal of Theoretical Biology*, **335**: 222–234.

[7] Vance, W., Ross, J., 1996. Fluctuations near limit cycles in chemical reaction systems. *The Journal of Chemical Physics*, **105**: 479–487.

[8] Boland, R. P., Galla, T., McKane, A. J., 2008. How limit cycles and quasi-cycles are related in systems with intrinsic noise. *Journal of Statistical Mechanics: Theory and Experiment*, P09001.

[9] Xiao, T., Ma, J., Hou, Z., Xin, H., 2007. Effects of internal noise in mesoscopic chemical systems near Hopf bifurcation. *New Journal of Physics*, **9**, 403.

[10] Borisuk, M. T., Tyson, J. J., 1998. Bifurcation Analysis of a Model of Mitotic Control in Frog Eggs. *Journal of Theoretical Biology*, **195**: 69–85.

[11] Schlögl , F., 1972. Chemical reaction models for nonequilibrium phase transition. *Z. Physik.*, **253**(**2**): 147–161.

[12] Érdi, P., Tóth, J. *Mathematical Models of Chemical Reactions. Theory and Applications of Deterministic and Stochastic Models.* Manchester University Press, Princeton University Press, 1989.

[13] Gaiko, V. A. *Global Bifurcation Theory and Hilbert's Sixteenth Problem.* Springer Science, 2003.

[14] Gaiko, V. A., 2009. On the Geometry of Polynomial Dynamical Systems. *Journal of Mathematical Sciences*, **157**(**3**): 400–412.

[15] Perko, L. M., 1984. Limit Cycles of Quadratic Systems in the Plane. *Rocky Mountain Journal of Mathematics*, **14**(**3**): 619–645.

[16] Cherkas, L. A., Artés, J. C., Llibre, J., 2003. Quadratic Systems with Limit Cycles of Normal Size. *Buletinul Academiei de Ştiinţe a Republicii Moldova. Matematica*, **1**(**41**): 31–46.

[17] Escher, C., 1981. Bifurcation and Coexistence of Several Limit Cycles in Models of Open Two-Variable Quadratic Mass-Action Systems. *Chemical Physics*, **63**: 337–348.

[18] Guidi, G. M., Goldbeter, A., 1997. Bistability without Hysteresis in Chemical Reaction Systems: A Theoretical Analysis of Irreversible Transitions between Multiple Steady States. *Journal of Physical Chemistry*, **101**: 9367–9376.

[19] Guidi, G. M., Goldbeter, A., 1998. Bistability without Hysteresis in Chemical Reaction Systems: The Case of Nonconnected Branches of Coexisting Steady States. *Journal of Physical Chemistry*, **102**: 7813–7820.

[20] Ghomi, M. S., Ciliberto, A., Kar, S., Novak, B., Tyson, J. J., 2008. Antagonism and Bistability in Protein Interaction Networks. *Journal of Theoretical Biology*, **218**: 209–218.

[21] Coppel, W., 1966. A Survey of Quadratic Systems. *Journal of Differential Equations*, **2**: 293–304.

[22] Chicone, C., Jinghuang, T., 1982. On General Properties of Quadratic Systems. *The American Mathematical Monthly*, **89**: 167–178.

[23] Perko, L. M. *Differential Equations and Dynamical Systems, Third Edition.* Springer-Verlag, New York, 2001.

[24] Dutt, A. K., 1992. Asymptotically Stable Limit Cycles in a Model of Glycolytic Oscillations. *Chemical Physics Letters*, **208**: 139–142.

[25] Kar, S., Baumann, W. T., Pau,l M. R. and Tyson, J. J., 2009. Exploring the Roles of Noise in the Eukaryotic Cell Cycle. *Proceedings of the National Academy of Sciences of USA*, **106**: 6471–6476.

[26] Vilar, J. M. G., Kueh, H. Y., Barkai, N. and Leibler, S., 2002. Mechanisms of Noise-resistance in Genetic Oscillators. *Proceedings of the National Academy of Sciences of the United States of America*, **99**(**9**): 5988–5992.

[27] Dickson, R. J., Perko, L. M., 1970. Bounded quadratic systems in the plane. *Journal of Differential Equations*, **7**: 251–273.

[28] Kuznetsov, Y. A. *Elements of Applied Bifurcation Theory, Second Edition.* Springer-Verlag, New York, 2000.

[29] Dublanche, Y., Michalodimitrakis, K., Kummerer, N., Foglierini, M. and Serrano, L., 2006. Noise in Transcription Negative Feedback Loops: Simulation and Experimental Analysis. *Molecular Systems Biology*, **2**(**41**): E1–E12.

[30] Bautin, N., 1954. On the number of limit cycles which appear with a variation of coefficients from an equilibrium position of focus or center type. *A.M.S. Translation*, **100**: 3–19.

[31] Han, M., Zhu, H., 2007. The loop quantities and bifurcations of homoclinic loops. *Journal of Differential Equations*, **234**: 339–359.

[32] Tóth, J., 1998. Multistationarity is neither necessary nor sufficient to oscillations. *Journal of Mathematical Chemistry*, **25**: 393–397.

[33] Escher, C., 1982. Double Hopf-Bifurcation in Plane Quadratic Mass-Action Systems. *Chemical Physics*, **67**: 239–244.

[34] Escher, C., 1979. Models of Chemical Reaction Systems with Exactly Evaluable Limit Cycle Oscillations. *Zeitschrift für Physik B*, **35**: 351–361.

[35] Tung, C-C., 1959. Positions of limit cycles of the system $\mathrm{d}x/\mathrm{d}t = \sum a_{ik}x^i y^k, \mathrm{d}y/\mathrm{d}t = \sum b_{ik}x^i y^k, 0 \leq i+k \leq 2$. *Sci. Sinica*, **8**: 151–171.

[36] Duff, G. D. F., 1953. Limit Cycles and Rotated Vector Fields. *Annals of Mathematics*, **67**: 15–31.

[37] Feinberg, M. *Lectures on Chemical Reaction Networks*, (Delivered at the Mathematics Research Center, U. of Wisconsin, 1979).

[38] Plesa, T., Zygalakis, K., Anderson, D. F., and Erban, R., 2016. The noise approximation algorithm. In preparation.